Steel and Composite Structures, *Vol. 19, No. 6 (2015) 1333-1354*
DOI: http://dx.doi.org/10.12989/scs.2015.19.6.1333

Higher order static analysis of truncated conical sandwich panels with flexible cores

Keramat Malekzadeh Fard*

Department of Structural Analysis and Simulation, Space research institute, Malek Ashtar University of Technology, Tehran-Karaj Highway, Post box: 14665-143, Tehran, Iran

(*Received May 24, 2014, Revised March 01, 2015, Accepted June 08, 2015*)

Abstract. A higher order analytical solution for static analysis of a truncated conical composite sandwich panel subjected to different loading conditions was presented in this paper which was based on a new improved higher order sandwich panel theory. Bending analysis of sandwich structures with flexible cores subjected to concentrated load, uniform distributed load on a patch, harmonic and uniform distributed loads on the top and/or bottom face sheet of the sandwich structure was also investigated. For the first time, bending analysis of truncated conical composite sandwich panels with flexible cores was performed. The governing equations were derived by principle of minimum potential energy. The first order shear deformation theory was used for the composite face sheets and for the core while assuming a polynomial description of the displacement fields. Also, the in-plane hoop stresses of the core were considered. In order to assure accuracy of the present formulations, convergence of the results was examined. Effects of types of boundary conditions, types of applied loads, conical angles and fiber angles on bending analysis of truncated conical composite sandwich panels were studied. As, there is no research on higher order bending analysis of conical sandwich panels with flexible cores, the results were validated by ABAQUS FE code. The present approach can be linked with the standard optimization programs and it can be used in the iteration process of the structural optimization. The proposed approach facilitates investigation of the effect of physical and geometrical parameters on the bending response of sandwich composite structures.

Keywords: static; truncated conical sandwich panels; improved higher order sandwich panel theory; point load; uniform distributed load on a patch

1. Introduction

Sandwich structures, owing to their high strength and stiffness and low weight and durability, are widely used in many engineering applications. These structures generally consist of two stiff face sheets and a soft core, which are bonded together. The advantages of this construction method are used to obtain the plates with high bending stiffness characteristics and extremely low weight.

Conical sandwich shells are often used as transition elements between cylinders of different diameters and/or end closures and sometimes as stand-alone components in various engineering applications such as tanks and pressure vessels, missiles and spacecraft, submarines, nuclear

*Corresponding author, Associate Professor, E-mail: k.malekzadeh@gmail.com

http://www.techno-press.org/?journal=scs&subpage=8 ISSN: 1229-9367 (Print), 1598-6233 (Online)

reactors, jet nozzles and other civil, chemical, mechanical, marine and aerospace engineering structures (Sofiyev 2011).

Based on Love's first-approximation shell theory, free vibration analysis of conical and cylindrical shells with various boundary conditions was performed by Wilkins *et al*. (1970). In their theory, transverse shear strain was not ignored. Using the finite deformation theory, Struk (1984) studied the buckling analysis of shallow open conical sandwich shells under uniform external pressure. Ren-huai and Jun (1995) performed non-linear free vibration analysis of shallow conical sandwich shells. They studied the effects of geometrical and physical parameters on free vibration response of shallow sandwich shell. In their theory the core and face sheets are transversely incompressible. Bardell *et al*. (1999) investigated a finite element vibration analysis of conical sandwich panels with different types of boundary conditions. They assumed that the core and face sheets were transversely incompressible. They also ignored the transverse shear strains in the face sheets. For bending analysis of sandwich structures, higher order sandwich panel theory was developed by Frostig and Shenar (1995), who considered two types of computational models in order to express the governing equations of the core. The second model assumed a polynomial description of the displacement fields in the core that was based on the displacement fields of the first model. Their theory did not impose any restrictions on the distribution of deformation through the core thickness. The improved higher order sandwich plate theory (IHSAPT), applying the first-order shear deformation theory for the face sheets, was introduced by Malekzadeh *et al*. (2005). Zhong and Reimerdes (2007) used a higher order theory and studied buckling analysis of cylindrical and conical sandwich shells with flexible core. Thermal and mechanical buckling of FG truncated conical shells based on the first-order shell theory and the Sanders nonlinear kinematics equations was done by Naj *et al*. (2008). Free vibration and buckling analyses of truncated conical shells with non-homogeneous material properties under uniform lateral and hydrostatic pressure were also done by Sofiyev *et al*. (2009). Biglari and Jafari (2010) presented a complex three layer theory for free vibration and bending analysis of open single curved sandwich structures. In their model, they used Donell's theory for the face sheets. Zhen and Wanji (2010) applied a C^0-type higher order equivalent single layer theory and investigated bending analysis of laminated composite and sandwich plates subjected to thermal and mechanical loads. Continuity conditions of transverse shear stresses at interfaces and conditions of zero transverse shear stresses on the upper and lower surfaces were also considered. Bending analysis of laminated composite plates under bi-sinusoidal loading using an equivalent single layer plate theory was done by Stürzenbecher and Hofstetter (2011). In their theory, transverse shear strains jumped at layer interfaces; but, transverse shear stresses were continuous and normal stress was ignored. Sofiyev (2011) studied non-linear buckling behavior of FG truncated conical shells subjected to a uniform axial compressive load based on 3D FEM. Bending analysis of FG conical panels was carried out by Aghdam *et al*. (2011), who used first-order shear deformation theory. Nedelcu (2011) investigated buckling behavior of isotropic conical shells under axial compression using generalized beam theory. Free vibration analysis of FG conical shell using meshless method and first-order shear deformation shell theory was done by Zhao and Liew (2011). Stürzenbecher *et al*. (2012) investigated bending analysis of sandwich panels with different core geometries including corrugated, honeycomb and X cores by neglecting transverse shear strains of the face sheets. Classical and first-order shear deformation theories were employed for the face sheets and core, respectively. Bich *et al*. (2012) studied linear buckling of FG truncated conical panels subjected to axial compression, external pressure and combination of these loads using the classical thin shell theory. Abediokhchi *et al*. (2013) investigated bending analysis of FG conical panels under transverse compression using first-order shear deformation theory and generalized differential quadrature method. The literature survey revealed that most of the researches have been performed on bending analysis of flat and curved composite sandwich panels and very little work has been carried out in the field of sandwich conical shells, most of which deal with buckling and vibration of isotropic, laminate and functionally graded (FG) conical shells. Therefore, there is no research on higher order bending analysis of conical sandwich panels with flexible cores. In addition, in these studies, the sandwich structures have been subjected to simple loadings while, in this paper, sandwich structures were subjected to multiple loading conditions including point load, uniform distributed load on a patch, harmonic and uniform distributed loads which were imposed on the top and/or bottom face sheets of the sandwich structure. Also, in this paper, using an improved higher order sandwich panel theory (Malekzadeh *et al*. 2005) and second computational model of Frostig (2004), bending analysis of conical composite sandwich panels was investigated. Also, the in-plane circumferential hoop stresses of the core were considered. Analytical solution of the displacement field of the core in terms of polynomials with unknown coefficients was presented according to the second computational model by Frostig and Thomsen (2004). Moreover, simply supported and fully clamped boundary conditions were considered. In order to assure accuracy of the present formulations, convergence of the results was examined in detail. Since there was few research on static bending analysis of a composite conical sandwich panel, to validate the obtained results, a conical sandwich panel was modeled in ABAQUS FE code and the results obtained from analytical formulations and FE code were compared with each other. Finally, effects of types of boundary conditions, types of applied loads, conical angles and fiber angles on static bending analysis of the truncated conical composite sandwich panels were studied.

2. Theoretical formulation

2.1 Basic assumptions

Consider a conical composite sandwich panel which is composed of two composite laminated face sheets. Thickness of the top face sheet, bottom face sheet and core is h_t, h_b and h_c, respectively, in which indices t and b refer to the top and bottom face sheets of the conical sandwich panel, respectively, as shown in Fig. 1. The assumption used in the present analysis is small deformation of linearly elastic materials. Conical apex angle is 2ϕ or 2α.

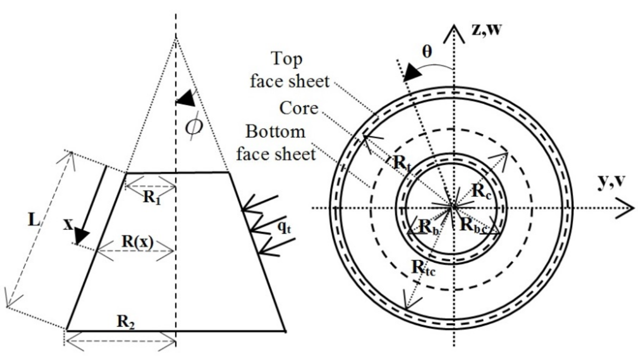

Fig. 1 Composite conical sandwich panel with laminated face sheets along with coordinates and dimensions of the panel

2.2 Kinematic relations

Base on the first shear deformation theory, the displacements u, v and w of the face sheets in the x, θ and z (thickness) directions are expressed through the following relations (Reddy 2004)

$$\begin{aligned} u_i(x,z,\theta) &= u_0^i(x,\theta,t) + z_i\psi_x^i(x,\theta) \\ v_i(x,z,\theta) &= v_0^i(x,\theta,t) + z_i\psi_\theta^i(x,\theta)\,; \quad (i=t,b) \\ w_i(x,z,\theta) &= w_0^i(x,\theta) \end{aligned} \tag{1}$$

where ψ_x^i and ψ_θ^i are rotation components of the transverse normal along x and θ-axes of the mid-surface of the top and bottom face-sheets. Also, u_0^i and v_0^i are displacement components in the x and θ directions, respectively, and w_0^i is vertical deflection of the top and bottom face-sheets. Z_i is vertical coordinate of the face-sheets which is measured upward from the mid-plane of the face-sheets (see Fig. 1). Kinematic equations for the strains in the face sheets are as follows (Qatu 2004)

$$\begin{aligned} &\varepsilon_{xx}^i = \varepsilon_{0xx}^i + z_i\kappa_{xx}^i\,,\ \varepsilon_{\theta\theta}^i = \varepsilon_{0\theta\theta}^i + z_i\kappa_{\theta\theta}^i, \varepsilon_{zz}^i = 0 \\ &\gamma_{x\theta}^i = 2\varepsilon_{x\theta}^i = \varepsilon_{0x\theta}^i + z_i\kappa_{x\theta}^i,\ \gamma_{xz}^i = 2\varepsilon_{xz}^i = \varepsilon_{0xz}^i\,, \gamma_{\theta z}^i = 2\varepsilon_{\theta z}^i = \varepsilon_{0\theta z}^i \quad ; \quad (i=t,b) \end{aligned} \tag{2}$$

where

$$\begin{aligned} &\varepsilon_{0xx}^i = \frac{\partial u_0^i}{\partial x}, \varepsilon_{0\theta\theta}^i = \frac{\partial v_0^i}{R_i(x)\partial\theta} + \frac{w_0^i\cos(\phi)}{R_i(x)} + \frac{u_0^i\sin(\phi)}{R_i(x)},\ \varepsilon_{0x\theta}^i = \frac{\partial v_0^i}{\partial x} + \frac{\partial u_0^i}{R_i(x)\partial\theta} - \frac{v_0^i\sin(\phi)}{R_i(x)}, \\ &\varepsilon_{0xz}^i = \frac{\partial w_0^i}{\partial x} + \psi_x^i, \varepsilon_{0\theta z}^i = \frac{\partial w_0^i}{R_i(x)\partial\theta} + \psi_\theta^i - \frac{v_0^i\cos(\phi)}{R_i(x)} \qquad ; \quad (i=t,b) \\ &\kappa_{xx}^i = \frac{\partial\psi_x^i}{\partial x}, \kappa_{\theta\theta}^i = \frac{\partial\psi_\theta^i}{R_i(x)\partial\theta}, \kappa_{x\theta}^i = \frac{\partial\psi_\theta^i}{\partial x} + \frac{\partial\psi_x^i}{R_i(x)\partial\theta} - \frac{\psi_\theta^i\sin(\phi)}{R_i(x)} \end{aligned} \tag{3}$$

and

$$R_i(x) = R_{i0} + x\sin(\phi); \quad (i=t,b) \tag{4}$$

The displacements fields are based on model II of Frostig (Frostig and Thomsen 2004) for the core and take a cubic pattern for the in-plane displacements and a quadratic one for the vertical displacement

$$\begin{cases} u_c(x,\theta,z) = u_0^c(x,\theta) + z_c u_1^c(x,\theta) + z_c^2 u_2^c(x,\theta) + z_c^3 u_3^c(x,\theta) \\ v_c(x,\theta,z) = (1+\dfrac{z}{R_c(x)})v_0^c(x,\theta) + z_c v_1^c(x,\theta) + z_c^2 v_2^c(x,\theta) + z_c^3 v_3^c(x,\theta) \\ w_c(x,\theta,z) = w_0^c(x,\theta) + z_c w_1^c(x,\theta) + z_c^2 w_2^c(x,\theta) \end{cases} \tag{5}$$

where u_k^c and v_k^c (k = 0, 1, 2, 3) are unknowns of the in-plane displacements of the core, respectively, and w_k^c (k = 0, 1, 2) are unknowns of its vertical displacements. $R_c(x)$ is the radius of curvature of the core in θ-z plane that varies with x

$$R_c(x) = R_{c0} + x\sin(\phi) \tag{6}$$

Kinematic relations of the core for a conical sandwich panel are

$$
\begin{aligned}
&\varepsilon_{xx}^{c}=\frac{\partial u_c}{\partial x},\quad \varepsilon_{\theta\theta}^{c}=\frac{1}{(1+z/R_c(x))}\left(\frac{\partial v_c}{a_2\partial\theta}+\frac{w_c}{R_c(x)}+\frac{u_c\partial a_2}{a_2\partial x}\right),\\
&\gamma_{x\theta}^{c}=2\varepsilon_{x\theta}^{c}=\frac{\partial v_c}{\partial x}+\frac{1}{(1+z/R_c(x))}\left(\frac{\partial u_c}{a_2\partial\theta}+\frac{v_c\partial a_2}{a_2\partial x}\right),\quad \gamma_{xz}^{c}=2\varepsilon_{xz}^{c}=\frac{\partial w_c}{\partial x}+\frac{\partial u_c}{\partial z},\\
&\gamma_{\theta z}^{c}=2\varepsilon_{\theta z}^{c}=\frac{1}{a_2(1+z/R_c(x))}\frac{\partial w_c}{\partial\theta}-\frac{v_c}{R_c^2(x)(1+z/R_c(x))}+\frac{\partial v_c}{\partial z}
\end{aligned}
\tag{7}
$$

where

$$
a_2=R_i(x)=R_{i0}+x\sin(\phi)\ ;\ \left(i=t,b,c\right) \tag{8}
$$

2.3 Governing equations

The equilibrium equations for the face sheets and core are derived using principle of minimum potential energy

$$
\delta\Pi=\delta U+\delta W_{ext}=0 \tag{9}
$$

where δU and δW_{ext} denote variations of strain energy and potential energy due to the applied loads, respectively. Also, δ denotes the variation operator.

The first variation of the internal potential energy for a composite conical sandwich panel including the top and bottom face sheets and core is

$$
\begin{aligned}
\delta U=&\sum_{i=t,b}\left(\int_{V_i}\left(\sigma_{xx}^{i}\delta\varepsilon_{xx}^{i}+\sigma_{\theta\theta}^{i}\delta\varepsilon_{\theta\theta}^{i}+\tau_{x\theta}^{i}\delta\gamma_{x\theta}^{i}+\tau_{xz}^{i}\delta\gamma_{xz}^{i}+\tau_{\theta z}^{i}\delta\gamma_{\theta z}^{i}\right)dV_i\right)\\
&+\int_{V_i}\left(\sigma_{xx}^{c}\delta\varepsilon_{xx}^{c}+\sigma_{\theta\theta}^{c}\delta\varepsilon_{\theta\theta}^{c}+\sigma_{zz}^{c}\delta\varepsilon_{zz}^{c}+\tau_{x\theta}^{c}\delta\gamma_{x\theta}^{c}+\tau_{xz}^{c}\delta\gamma_{xz}^{c}+\tau_{\theta z}^{c}\delta\gamma_{\theta z}^{c}\right)dV_c
\end{aligned}
\tag{10}
$$

The variation of the external work is sum of the applied loads on the top and bottom face sheets

$$
\delta W_{ext}=\int_A\left(-(1+\frac{h_t}{2R_t(x)})q_t\delta w_0^t+(1-\frac{h_b}{2R_b(x)})q_b\delta w_0^b\right)dA \tag{11}
$$

Using the principle of minimum potential energy (Eqs. (9)-(11)) and kinematic relations (Eqs. (1)-(8)), the governing equations can be obtained as

$$
\begin{aligned}
&\frac{\partial N_{xx}^{t}}{\partial x}+\frac{(N_{xx}^{t}-N_{\theta\theta}^{t})\sin(\phi)}{R_t(x)}+\frac{\partial N_{x\theta}^{t}}{R_t(x)\partial x_\theta}+\frac{2}{h_c^2}M_{2xx,x}^{c}+\frac{2}{R_c(x)h_c^2}\sin(\phi)M_{2xx}^{c}+\frac{4}{h_c^3}M_{3xx,x}^{c}+\\
&\frac{4}{R_c(x)h_c^3}\sin(\phi)M_{3xx}^{c}-\frac{2}{R_c(x)h_c^2}\sin(\phi)M_{2\theta\theta}^{c}-\frac{4}{R_c(x)h_c^3}\sin(\phi)M_{3\theta\theta}^{c}+\frac{2}{R_c(x)h_c^2}M_{2\theta x,\theta}^{c}+\\
&\frac{4}{R_c(x)h_c^3}M_{3\theta x,\theta}^{c}-\frac{4}{h_c^2}M_{1xz}^{*c}-\frac{12}{h_c^3}M_{2xz}^{*c}=0
\end{aligned}
\tag{12}
$$

$$\frac{\partial N_{xx}^{b}}{\partial x}+\frac{(N_{xx}^{b}-N_{\theta\theta}^{b})\sin(\phi)}{R_b(x)}+\frac{\partial N_{x\theta}^{b}}{R_b(x)\partial x_\theta}+\frac{2}{h_c^2}M_{2xx,x}^{c}+\frac{2}{h_c^2}\sin(\phi)M_{2xx}^{c}-\frac{4}{h_c^3}M_{3xx,x}^{c}-$$
$$\frac{4}{h_c^3}\sin(\phi)M_{3xx}^{c}+\frac{2}{R_c(x)h_c^2}M_{2\theta x,\theta}^{c}-\frac{2}{R_c(x)h_c^2}\sin(\phi)M_{2\theta\theta}^{c}+\frac{4}{R_c(x)h_c^3}\sin(\phi)M_{3\theta\theta}^{c}- \quad (13)$$
$$\frac{4}{R_c(x)h_c^3}M_{3\theta x,\theta}^{c}-\frac{4}{h_c^2}M_{1xz}^{*c}+\frac{12}{h_c^3}M_{2xz}^{*c}=0$$

$$\frac{\partial N_{x\theta}^{t}}{\partial x}+\frac{\partial N_{\theta\theta}^{t}}{R_t(x)\partial x_\theta}+\frac{Q_{\theta z}^{t}\cos(\phi)}{R_t(x)}+\frac{2}{R_c(x)h_c^2}M_{2\theta\theta,\theta}^{c}+\frac{4}{R_c(x)h_c^3}M_{3\theta\theta,\theta}^{c}+\frac{2}{h_c^2}M_{2x\theta,x}^{c}+$$
$$\frac{2}{R_c(x)h_c^2}\sin(\phi)M_{2x\theta}^{c}+\frac{4}{h_c^3}M_{3x\theta,x}^{c}+\frac{4}{R_c(x)h_c^3}\sin(\phi)M_{3x\theta}^{c}+\frac{2}{R_c(x)h_c^2}\sin(\phi)M_{2\theta x}^{c}+ \quad (14)$$
$$\frac{4}{R_c(x)h_c^3}\sin(\phi)M_{3\theta x}^{c}+\frac{2}{R_c(x)h_c^2}M_{2\theta z}^{c}+\frac{4}{R_c(x)h_c^3}M_{3\theta z}^{c}-\frac{4}{h_c^2}M_{1\theta z}^{*c}-\frac{12}{h_c^3}M_{2\theta z}^{*c}=0$$

$$\frac{\partial N_{x\theta}^{b}}{\partial x}+\frac{\partial N_{\theta\theta}^{b}}{R_b(x)\partial x_\theta}+\frac{Q_{\theta z}^{b}\cos(\phi)}{R_b(x)}+\frac{\partial N_{x\theta}^{b}}{\partial x}+\frac{\partial N_{\theta\theta}^{b}}{R_b(x)\partial x_\theta}+\frac{Q_{\theta z}^{b}\cos(\phi)}{R_b(x)}++\frac{2}{R_c h_c^2}M_{2\theta\theta,\theta}^{c}+\frac{2}{h_c^2}M_{2x\theta,x}^{c}$$
$$-\frac{4}{R_c h_c^3}M_{3\theta\theta,\theta}^{c}+\frac{2}{R_c(x)h_c^2}\sin(\phi)M_{2x\theta}^{c}-\frac{4}{R_c(x)h_c^3}\sin(\phi)M_{3x\theta}^{c}-\frac{4}{h_c^3}M_{3x\theta,x}^{c}+\frac{2}{R_c(x)h_c^2}\sin(\phi)M_{2\theta x}^{c} \quad (15)$$
$$-\frac{4}{R_c(x)h_c^3}\sin(\phi)M_{3\theta x}^{c}+\frac{2}{R_c(x)h_c^2}M_{2\theta z}^{c}-\frac{4}{R_c(x)h_c^3}M_{3\theta z}^{c}-\frac{4}{h_c^2}M_{1\theta z}^{*c}+\frac{12}{h_c^3}M_{2\theta z}^{*c}=0$$

$$\frac{\partial Q_{xz}^{t}}{\partial x}+\frac{\partial Q_{\theta z}^{t}}{R_t(x)\partial x_\theta}+\frac{\partial Q_{xz}^{t}\sin(\phi)}{\partial x}-\frac{N_{\theta\theta}^{t}\cos(\phi)}{R_t(x)}-\frac{R_z^c}{h_c}-\frac{4}{h_c^2}M_z^c-\frac{1}{R_c(x)h_c}M_{1\theta\theta}^{c}$$
$$\frac{2}{R_c(x)h_c^2}M_{2\theta\theta}^{c}+\frac{1}{h_c}M_{1xz,x}^{c}+\frac{1}{R_c(x)h_c}\sin(\phi)M_{1xz}^{c}+\frac{2}{h_c^2}M_{2xz,x}^{c}+\frac{2}{R_c(x)h_c^2}\sin(\phi)M_{2xz}^{c}+ \quad (16)$$
$$\frac{1}{R_c h_c}M_{1\theta z,\theta}^{c}+\frac{2}{R_c h_c^2}M_{2\theta z,\theta}^{c}-(1+\frac{h_t}{2R_t(x)})q_t=0$$

$$\frac{\partial Q_{xz}^{b}}{\partial x}+\frac{\partial Q_{\theta z}^{b}}{R_b(x)\partial x_\theta}+\frac{\partial Q_{xz}^{b}\sin(\phi)}{\partial x}-\frac{N_{\theta\theta}^{b}\cos(\phi)}{R_b(x)}+\frac{R_z^c}{h_c}+\frac{1}{R_c h_c}M_{1\theta\theta}^{c}-\frac{2}{R_c h_c^2}M_{2\theta\theta}^{c}-$$
$$\frac{1}{h_c}M_{1xz,x}^{c}-\frac{4}{h_c^2}M_z^c-\frac{1}{R_c(x)h_c}\sin(\phi)M_{1xz}^{c}+\frac{2}{h_c^2}M_{2xz,x}^{c}+\frac{2}{R_c(x)h_c^2}\sin(\phi)M_{2xz}^{c}-\frac{1}{h_c}M_{1\theta z,\theta}^{c} \quad (17)$$
$$+\frac{2}{h_c^2}M_{2\theta z,\theta}^{c}+(1-\frac{h_b}{2R_b(x)})q_b=0$$

$$\frac{\partial M_{xx}^{t}}{\partial x}+\frac{\partial M_{x\theta}^{t}}{R_t(x)\partial x_\theta}+\frac{(M_{xx}^{t}-M_{\theta\theta}^{t})\sin(\phi)}{R_t(x)}-Q_{xz}^{t}-\frac{h_t}{h_c^2}M_{2xx,x}^{c}-\frac{h_t}{R_c(x)h_c^2}\sin(\phi)M_{2xx}^{c}$$
$$-\frac{2h_t}{h_c^3}M_{3xx,x}^{c}-\frac{2h_t}{R_c(x)h_c^3}\sin(\phi)M_{3xx}^{c}-\frac{h_t}{R_c h_c^2}M_{2\theta x,\theta}^{c}-\frac{2h_t}{R_c h_c^3}M_{3\theta x,\theta}^{c}+\frac{2h_t}{h_c^2}M_{1xz}^{*c}+\frac{6h_t}{h_c^3}M_{2xz}^{*c} \quad (18)$$
$$+\frac{h_t}{R_c(x)h_c^2}\sin(\phi)M_{2\theta\theta}^{c}+\frac{h_t}{R_c(x)h_c^3}\sin(\phi)M_{3\theta\theta}^{c}=0$$

$$\frac{\partial M^b_{xx}}{\partial x}+\frac{\partial M^b_{x\theta}}{R_b(x)\partial x_\theta}+\frac{(M^b_{xx}-M^b_{\theta\theta})\sin(\phi)}{R_b(x)}-Q^b_{xz}+\frac{h_b}{h_c^2}M^c_{2xx,x}+\frac{h_t}{R_c(x)h_c^2}\sin(\phi)M^c_{2xx}-\frac{2h_b}{h_c^3}M^c_{3xx,x}-\frac{2h_t}{R_c(x)h_c^3}\sin(\phi)M^c_{3xx}-\frac{h_b}{R_c h_c^2}M^c_{2\theta x,\theta}-\frac{2h_b}{R_c h_c^3}M^c_{3\theta x,\theta}-\frac{2h_b}{h_c^2}M^{*c}_{1xz}+\frac{6h_b}{h_c^3}M^{*c}_{2xz}-\frac{h_t}{R_c(x)h_c^2}\sin(\phi)M^c_{2\theta\theta}+\frac{h_t}{R_c(x)h_c^3}\sin(\phi)M^c_{3\theta\theta}=0 \tag{19}$$

$$\frac{\partial M^t_{x\theta}}{\partial x}+\frac{\partial M^t_{\theta\theta}}{R_t(x)\partial x_\theta}+\frac{2M^t_{x\theta}\sin(\phi)}{R_t(x)}-Q^t_{\theta z}-\frac{h_t}{R_c(x)h_c^2}M^c_{2\theta\theta,\theta}-\frac{2h_t}{R_c(x)h_c^3}M^c_{3\theta\theta,\theta}-\frac{h_t}{h_c^2}M^c_{2x\theta,x}-\frac{h_t}{R_c(x)h_c^2}\sin(\phi)M^c_{2x\theta}-\frac{2h_t}{h_c^3}M^c_{3x\theta,x}-\frac{2h_t}{R_c(x)h_c^3}\sin(\phi)M^c_{3x\theta}+\frac{2h_t}{h_c^2}M^{*c}_{1\theta z}+\frac{6h_t}{h_c^3}M^{*c}_{2\theta z}-\frac{h_t}{R_c(x)h_c^2}\sin(\phi)M^c_{2\theta x}-\frac{2h_t}{R_c(x)h_c^3}\sin(\phi)M^c_{3\theta x}=0 \tag{20}$$

$$\frac{\partial M^b_{x\theta}}{\partial x}+\frac{\partial M^b_{\theta\theta}}{R_b(x)\partial x_\theta}+\frac{2M^b_{x\theta}\sin(\phi)}{R_b(x)}-Q^b_{\theta z}+\frac{h_b}{R_c(x)h_c^2}M^c_{2\theta\theta,\theta}-\frac{2h_b}{R_c(x)h_c^3}M^c_{3\theta\theta,\theta}+\frac{h_b}{h_c^2}M^c_{2x\theta,x}+\frac{h_t}{R_c(x)h_c^2}\sin(\phi)M^c_{2x\theta}-\frac{2h_b}{h_c^3}M^c_{3x\theta,x}+\frac{2h_t}{R_c(x)h_c^3}\sin(\phi)M^c_{3x\theta}-\frac{h_b}{R_c(x)h_c^2}M^c_{2\theta z}-\frac{2h_b}{R_c(x)h_c^2}M^c_{3\theta z}-\frac{2h_b}{h_c^2}M^{*c}_{1\theta z}+\frac{6h_b}{h_c^3}M^{*c}_{2\theta z}+\frac{h_t}{R_c(x)h_c^2}\sin(\phi)M^c_{2\theta x}-\frac{2h_t}{R_c(x)h_c^3}\sin(\phi)M^c_{3\theta x}=0 \tag{21}$$

$$N^c_{xx,x}+\frac{1}{R_c(x)}\sin(\phi)N^c_{xx,x}+\frac{1}{R_c}N^c_{\theta x,\theta}-\frac{4}{h_c^2}M^c_{2xx,x}-\frac{4\sin(\phi)}{R_c(x)h_c^2}M^c_{2xx}-\frac{4}{R_c h_c^2}M^c_{2\theta x,\theta}+\frac{8}{h_c^2}M^{*c}_{1xz}-\frac{1}{R_c(x)}\sin(\phi)N^c_{\theta\theta}+\frac{4}{h_c^2R_c(x)}\sin(\phi)M^c_{2\theta\theta}=0 \tag{22}$$

$$M^c_{1xx,x}+\frac{\sin(\phi)}{R_c(x)}M^c_{1xx}-N^{*c}_{xz}-\frac{4}{h_c^2}M^c_{3xx,x}-\frac{4\sin(\phi)}{R_c(x)h_c^2}M^c_{3xx}+\frac{1}{R_c(x)}M^c_{1\theta x,\theta}-\frac{4}{R_c(x)h_c^2}M^c_{3\theta x,\theta}+\frac{12}{h_c^2}M^{*c}_{2xz}-\frac{\sin(\phi)}{R_c(x)}M^c_{1\theta\theta}+\frac{4\sin(\phi)}{h_c^2R_c(x)}M^c_{3\theta\theta}=0 \tag{23}$$

$$\frac{1}{R_c(x)}N^c_{\theta\theta,\theta}+N^c_{x\theta,x}+\frac{1}{R_c(x)}\sin(\phi)N^c_{x\theta}-\frac{4}{R_c(x)h_c^2}M^c_{2\theta\theta,\theta}-\frac{4}{R_c^2(x)h_c^2}M^c_{3\theta\theta,\theta}+\frac{1}{R_c(x)}M^c_{1x\theta,x}-\frac{4}{h_c^2}M^c_{2x\theta,x}-\frac{4}{R_c(x)h_c^2}\sin(\phi)M^c_{2x\theta}-\frac{4}{R_c(x)h_c^2}M^c_{3x\theta,x}+\frac{1}{R_c(x)}\sin(\phi)N^c_{\theta x}+\frac{1}{R_c^2(x)}\sin(\phi)M^c_{1\theta x}+\frac{1}{R_c(x)}N^c_{\theta z}--\frac{4}{R_c(x)h_c^2}\sin(\phi)M^c_{2\theta x}-\frac{4}{R_c^2(x)h_c^2}\sin(\phi)M^c_{3\theta x}\frac{4}{R_c(x)h_c^2}M^c_{2\theta z}-\frac{4}{R_c^2(x)h_c^2}M^c_{3\theta z}+\frac{8}{h_c^2}M^{*c}_{1\theta z}+\frac{12}{R_c(x)h_c^2}M^{*c}_{2\theta z}-\frac{1}{R_c(x)}N^{*c}_{\theta z}=0 \tag{24}$$

$$
\begin{aligned}
&\frac{1}{R_c(x)}M^c_{1\theta\theta,\theta}-N^{*c}_{\theta z}-\frac{4}{R_c(x)h_c^2}M^c_{3\theta\theta,\theta}+M^c_{1x\theta,x}+\frac{1}{R_c(x)}\sin(\phi)M^c_{1x\theta}-\frac{4}{h_c^2R_c(x)}\sin(\phi)M^c_{3x\theta}\\
&-\frac{4}{h_c^2}M^c_{3x\theta,x}+\frac{1}{R_c(x)}\sin(\phi)M^c_{1\theta x}-\frac{4}{h_c^2R_c(x)}\sin(\phi)M^c_{3\theta x}+\frac{1}{R_c(x)}M^c_{1\theta z}-\frac{4}{R_c(x)h_c^2}M^c_{3\theta z}+\frac{12}{h_c^2}M^{*c}_{2\theta z}=0
\end{aligned}
\tag{25}
$$

$$
\begin{aligned}
&N^c_{xz,x}+\frac{\sin(\phi)}{R_c(x)}N^c_{xz}+\frac{1}{R_c(x)}N^c_{\theta z,\theta}+\frac{8}{h_c^2}M^c_z-\frac{1}{R_c(x)}N^c_{\theta\theta}+\frac{4}{R_c(x)h_c^2}M^c_{2\theta\theta}-\frac{4}{h_c^2}M^c_{2xz,x}\\
&-\frac{4}{h_c^2}\frac{\sin(\phi)}{R_c(x)}M^c_{2xz}-\frac{4}{R_c(x)h_c^2}M^c_{2\theta z,\theta}=0
\end{aligned}
\tag{26}
$$

where stress resultants per unit length can be defined. They were shown in appendix A. Also using the principle of minimum potential energy (Eqs. (9)-(11)) and kinematic relations (Eqs. (1)-(8)), the boundary conditions equations can be obtained. The simply supported geometrical and physical boundary conditions for a truncated conical shell at the edges x = 0, a of the top, bottom face-sheets and the core are

$$
\begin{aligned}
&N^i_{xx}=0\ or\ u^i_0=0,\ N^i_{x\theta}=0\ or\ v^i_0=0,\ M^i_{xx}=0\ or\ \psi^i_x=0,\ M^i_{x\theta}=0\ or\ \psi^i_\theta=0,\\
&Q^i_{xz}=0\ or\ w^i_0=0,\ M^c_{1xz}=0\ or\ w^i_0=0,\ N^c_{xx}=0\ or\ u^c_0=0,\ M^c_{1xx}=0\ or\ u^c_1=0,\\
&M^c_{2xx}=0\ or\ u^c_2=0,\ M^c_{3xx}=0\ or\ u^c_3=0,\ N^c_{x\theta}=0\ or\ v^c_0=0,\ M^c_{1x\theta}=0\ or\ v^c_1=0,\\
&M^c_{2x\theta}=0\ or\ v^c_o=0,\ M^c_{3x\theta}=0\ or\ v^c_0=0,\ N^c_{xz}=0\ or\ w^c_0=0\ \ ;\ i=t,b.
\end{aligned}
\tag{27}
$$

3. Analytical solution

The displacement field based on double Fourier series for a conical composite sandwich panel with simply supported boundary conditions at the top and bottom face-sheets was assumed to be in the following form

$$
\begin{bmatrix} u^j_0(x,\theta)\\ v^j_0(x,\theta)\\ w^j_0(x,\theta)\\ \psi^j_x(x,\theta)\\ \psi^j_\theta(x,\theta)\\ u^c_k(x,\theta)\\ v^c_k(x,\theta)\\ w^c_l(x,\theta)\end{bmatrix}=\sum_{n=0}^{\infty}\sum_{m=1}^{\infty}\begin{bmatrix} U^j_{0mn}\cos(\alpha_m x)\cos(n\theta)\\ V^j_{0mn}\sin(\alpha_m x)\sin(n\theta)\\ W^j_{0mn}\sin(\alpha_m x)\cos(n\theta)\\ \Psi^j_{xmn}\cos(\alpha_m x)\cos(n\theta)\\ \Psi^j_{\theta mn}\sin(\alpha_m x)\sin(n\theta)\\ U^c_{kmn}\cos(\alpha_m x)\cos(n\theta)\\ V^c_{kmn}\sin(\alpha_m x)\sin(n\theta)\\ W^c_{lmn}\sin(\alpha_m x)\cos(n\theta)\end{bmatrix},\ \text{(k=0,1,2,3), (l=0,1,2)}
\tag{28}
$$

where U^j_{0mn}, V^j_{0mn}, W^j_{0mn}, Ψ^j_{xmn}, $\Psi^j_{\theta mn}$, U^c_{kmn}, V^c_{kmn} and W^c_{lmn} are Fourier coefficients and m and n are half wave numbers along x and θ directions, respectively. The above double Fourier series functions can satisfy simply supported boundary condition on all edges for a conical composite sandwich panel. However, when all edges are clamped, only the function cos$\alpha_m x$ in the above series expansions must be replaced with sin$\alpha_m x$.

In Eqs. (16)-(17), the static loads (q_j (j = t, b)) normal to the top and/or the bottom face sheets of a conical composite sandwich are assumed to be represented by series expansion as follows

$$q_j(x,\theta)=\sum_{m=1}^{\infty}\sum_{n=0}^{\infty} q_{mn}^{j}\sin(\alpha_m x)\cos(n\theta)\ ;\ j=t,b \tag{29}$$

Where q_{mn} is Fourier coefficient that is dependent on types of loads. Fourier coefficient for the uniform distributed load on the top and/or bottom face sheets of the conical sandwich panel can be obtained as follows

$$\begin{cases} q_{m0}^{j}=\dfrac{1}{\pi L}\displaystyle\int_0^L\int_0^{2\pi} q_j(x,\theta)(\sin\alpha_m x)dx\,d\theta \\ q_{mn}^{j}=\dfrac{2}{\pi L}\displaystyle\int_0^L\int_0^{2\pi} q_j(x,\theta)(\sin\alpha_m x)(\cos n\theta)dx\,d\theta \end{cases} \quad \text{where } q_j(x,\theta)=q_0\ ;\ j=t,b \Rightarrow$$
$$\begin{cases} q_{m0}^{j}=\dfrac{4q_0}{m\pi} & \text{for } m=1,3,5,... \\ q_{m0}^{j}=0 & \text{for } m=2,4,6,... \\ q_{mn}^{j}=0 & for\ n>0 \end{cases} \tag{30}$$

For the point load acting on an arbitrary point (x_i, θ_i) can be determined as follows

$$\begin{cases} q_{m0}^{j}=\dfrac{1}{\pi L}\displaystyle\int_0^L\int_0^{2\pi} q_j(x,\theta)(\sin\alpha_m x)dx\,d\theta \\ q_{mn}^{j}=\dfrac{2}{\pi L}\displaystyle\int_0^L\int_0^{2\pi} q_j(x,\theta)(\sin\alpha_m x)(\cos n\theta)dx\,d\theta \end{cases} \quad \text{where} q_j(x,\theta)=q_0\delta(x-x_i)\delta(\theta-\theta_i);j=t,b \Rightarrow$$
$$\begin{cases} q_{m0}^{j}=\dfrac{q_0}{\pi LR}\sin(\alpha_m x_i) \\ q_{mn}^{j}=\dfrac{2q_0}{\pi LR}\sin(\alpha_m x_i)\cos(n\theta_i) \qquad for\ n>0 \end{cases} \tag{31}$$

For the uniform static load distributed on the patch with length $2L_1$ ($R(\theta_2-\theta_1)=2L_1$)) and width $2L_2$ ($R(x_2-x_1)=2L_2$)), the applied load was assumed to be only in the radial direction over a small rectangular area ($2L_1 \times 2L_2$) and other external excitations were neglected. Constant Fourier coefficients q_{mn}^{j} could be determined as follows

$$\begin{cases} q_{m0}^{j}=\dfrac{1}{\pi L}\displaystyle\int_{x_1}^{x_2}\int_{\theta_1}^{\theta_2} q_j(x,\theta)(\sin\alpha_m x)dx\,d\theta \\ q_{mn}^{j}=\dfrac{2}{\pi L}\displaystyle\int_{x_1}^{x_2}\int_{\theta_1}^{\theta_2} q_j(x,\theta)(\sin\alpha_m x)(\cos n\theta)dx\,d\theta \end{cases} \quad \text{where } q_j(x,\theta)=q_0;\ j=t,b \Rightarrow$$
$$\begin{cases} q_{m0}^{j}=\dfrac{q_0}{m\pi^2}[\cos(\alpha_m x_1)-\cos(\alpha_m x_2)](\theta_2-\theta_1) \\ q_{mn}^{j}=\dfrac{2q_0}{mn\pi^2}[\cos(\alpha_m x_1)-\cos(\alpha_m x_2)](\sin(n\theta_2)-\sin(n\theta_1)) \quad for\ n>0 \end{cases} \tag{32}$$

For the harmonic load on the top and/or bottom face sheets, they can be determined as follows

$$\begin{cases} q_{m0}^{j} = \dfrac{1}{\pi L}\int_0^L\int_0^{2\pi} q_j\left(x,\theta\right)\left(\sin\alpha_m x\right)dx\,d\theta \\ q_{mn}^{j} = \dfrac{2}{\pi L}\int_0^L\int_0^{2\pi} q_j\left(x,\theta\right)\left(\sin\alpha_m x\right)\left(\cos n\theta\right)dx\,d\theta \end{cases} \quad \text{where } q_j\left(x,\theta\right) = q_0\left(\sin\frac{\pi}{L}x\right)\left(\cos\theta\right);\ j = t,b \Rightarrow \tag{33}$$

$$\begin{cases} q_{m0}^{j} = 0, & m = 1,\ n = 0 \\ q_{mn}^{j} = q_0, & m = 1,\ n = 1 \end{cases}$$

Therefore, the governing equation of motion to the static bending analysis of conical composite sandwich panel can be written as follows

$$\begin{gathered} [K]\{c\} = \{Q\} \\ \{c\} = \{U_{0mn}^{t}, U_{0mn}^{b}, V_{0mn}^{t}, V_{0mn}^{b}, W_{0mn}^{t}, W_{0mn}^{b}, \psi_{xmn}^{t}, \psi_{xmn}^{b}, \psi_{\theta mn}^{t}, \psi_{\theta mn}^{b}, U_{0mn}^{c}, V_{0mn}^{c}, U_{1mn}^{c}, V_{1mn}^{c}, W_{0mn}^{c}\}^{T} \\ \{Q\} = \{0,0,0,0,-q_{mn}^{t}, q_{mn}^{b}, 0,0,0,0,0,0,0,0,0\}^{T} \end{gathered} \tag{34}$$

where some coefficients of stiffness matrix [K] $(15\,\mathrm{m}\,(n+1))\times(15\,\mathrm{m}\,(n+1))$ are given in Appendix B which for SS B.C. and [Q] is $(15\,\mathrm{m}\,(n+1))\times(1)$ vector of the arbitrary static force or forces.

4. Results and discussion

In this section, some examples are considered and the obtained results are validated and discussed. In order to demonstrate their capability in predicting static bending analysis of a composite conical sandwich panel, some examples are presented. Since there has been no research on static bending analysis of a composite conical sandwich panel for validating the obtained results, a conical sandwich panel was modeled in ABAQUS FE code and the results obtained from analytical formulations and FE code were compared with each other. The agreement between the results was very good.

Example 1:
Static bending analysis of a composite conical sandwich panel with SS and CC B.Cs.

In this example static bending of a composite conical sandwich panel was studied. Properties of the conical structure are given in Table 1. It is assumed that static load (q_0) was uniformly applied to the area (UAL) (A = 2L_1 × 2L_2, L_1 = L_2 = L/8), uniformly (UDL) and harmonically (SSL) distributed loads on the top (outer) face sheet of the sandwich structure. In Table 2, convergence of

Table 1 Material properties of a conical composite sandwich panel

Foam core	Composite face sheets
$E_1 = E_2 = E_3 = 0.1036$ GPa, $G_{12} = G_{13} = G_{23} = 0.05$ GPa, $v = 0.036$, $\rho = 130$ kg/m^3	$E_1 = 131$ GPa, $E_2 = 10.34$ GPa, $G_{12} = G_{13} = 6.895$ GPa, $G_{23} = 6.205$ GPa, $v_{12} = 0.22$, $\rho = 1627$kg/m^3

Geometrical properties: $h_c/h = 0.88$, $R_{c1} = 10h$, $L = R_{c1}$, [0 90 0 / core / 0 90 0], $\varphi = 30°$

Table 2 Convergence of dimensionless deflection at the center of top face sheet of a composite conical sandwich panel subjected to the UDL, SSL and UAL on the top face sheet

$w^* = 100 W_t h^3 E_{2t} / (q_0 R_{1t}^4)$						
Convergence ($m = n$)	S.S. Boundary conditions			C.C. Boundary conditions		
3	3.8795	5.6458	3.3204	5.3371	5.7150	1.9690
5	3.7891	5.6550	3.3873	5.8505	5.6392	3.8058
9	3.5693	5.6685	3.3922	6.1208	5.5724	5.6741
13	3.6217	5.6822	3.4411	6.2079	5.5632	6.2193
15	3.6131	5.6887	3.4643	6.2467	5.5664	6.3258
17	3.6129	5.6889	3.4645	6.2469	5.5665	6.3259

Table 3 Comparing dimensionless central deflection of a composite conical sandwich panel subjected to the area load (UAL)

$w^* = 100 W_t h^3 E_{2t} / (q_0 R_{1t}^4),\quad L\sin(\varphi) = 0.5 R_{1t},\quad \varphi = 30^\circ$			
B.Cs.	Present model	ABAQUS	Maximum error (%)
S.S.	3.6129	3.3683	6.77
C.C.	6.2469	6.0192	3.64

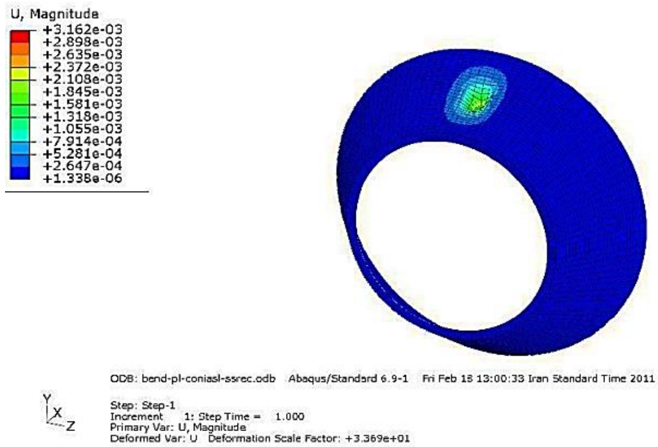

Fig. 2 The 3D view of the deflection of a composite conical sandwich panel with S.S. B.Cs. subjected to area load

the dimensionless central deflection for both boundary conditions is presented. In this example, 30 MPa was considered for values of all the applied loads. It can be seen from Table 2, central deflection for all the applied loads converged after 225 expressions ($m = n = 15$).

In Table 3, results of the presented formulations are validated using results of ABAQUS analysis. In this study, composite conical sandwich panel with foam core was meshed using SC8R elements. In the finite element model presented in this study, the motion of the face sheet is related to the motion of the core through constraint equations utilizing the concept of slave and master nodes. The finite element model is capable of taking transverse flexibility into consideration. In particular, certain boundary conditions which may not be studied analytically can be studied using the present finite element model. This table showed little difference between the results and the presented formulations was in very good agreement with FE results. The 3D view of deflection of a conical structure subjected to the area load obtained from ABAQUS code for simply supported boundary conditions (S.S. B.Cs.) is presented in Fig. 2. Also, 3D view of the dimensionless deflection of a composite conical sandwich structure subjected to the area and harmonic loads for S.S. B.Cs. is given in Fig 3. These results obtained from the present analytical solution.

Example 2: *Effect of conical angle on static response of a composite conical sandwich panel*

In this example, effect of conical angle on the static response of a composite conical sandwich panel subjected to uniformly (UDL) and harmonically (SSL) distributed loads with S.S. and C.C. B.Cs. was investigated. Mechanical and geometrical properties of the composite conical sandwich panel are given in Table 4. Variations of the face sheet deflections with conical angles for a composite conical sandwich panel subjected to SSL and UDL with S.S. B.Cs. at $(x, \theta, z_i) = (L/2, 0, h_i/2)$, $(i = t, b)$ are presented in Fig. 4. With increasing the conical angle, the dimensionless deflections of the top (outer) and bottom (inner) face sheets in all the cases increased and, in all the cases, increasing rates of deflection were approximately equal, as shown in Fig. 4. Moreover, for both load conditions, the top and bottom face sheet deflections subjected to SSL were higher than

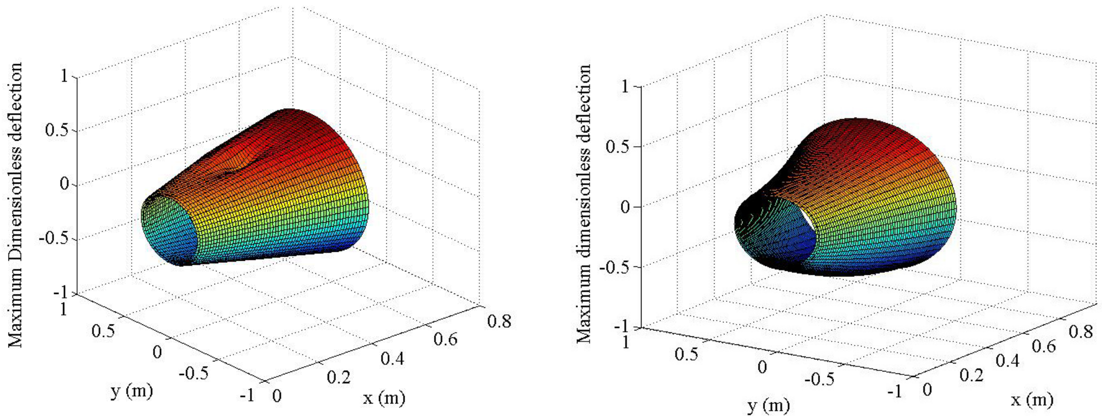

(a) UAL, S.S. B.Cs. (b) SSL, S.S. B.Cs.

Fig. 3 The 3D view of the dimensionless deflection of a composite conical sandwich panel with S.S. B.Cs. subjected to the area and the harmonic loads (Sinusoidal load)

Table 4 Mechanical and geometrical properties of a conical composite sandwich panel

Foam core	$E_1 = E_2 = E_3 = 0.1036$ GPa, $G_{12} = G_{13} = G_{23} = 0.05$ GPa, $\nu = 0.036$, $\rho = 130$ kb/m^3
Composite face sheets	$E_1 = 131$ GPa, $E_2 = 10.34$ GPa, $G_{12} = G_{13} = 6.895$ GPa, $G_{23} = 6.205$ GPa, $\nu_{12} = 0.22$, $\rho = 1627$ kb/m^3
Geometry	$h_c/h = 0.88$, $R_{c1} = 10h$, $L = R_{c1}$, [0 90 0 / core / 0 90 0]

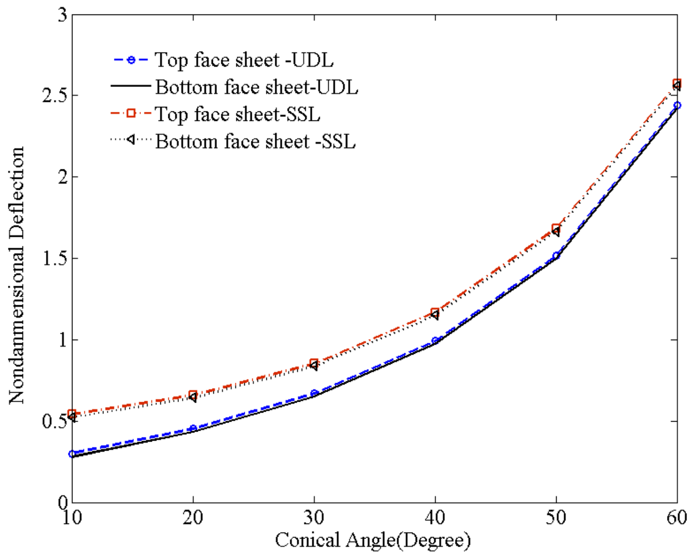

Fig. 4 Variation of the dimensionless face sheet deflections with the conical angles for UDL and SSL loads at (x, θ, z_i) = (L/2, 0, h_i/2), (i = t, b)

those subjected to UDL. The dimensionless deflection at the center of the bottom face sheet was lower than that at the center of the top face sheet because, in the current method, flexibility of the core was modeled and caused deflections of the top and bottom face sheets to be different.

Variations of the transverse normal stress of the core with the conical angle for a composite conical sandwich panel subjected to SSL and UDL with S.S. B.Cs. at (x, θ, z_c) = (L/2, 0, h_c/2) are presented in Fig. 5. This figure shows that increasing the conical angle caused those values of the transverse normal stresses of the core in both cases to increase. Also, increasing rate of this value for SSL was much higher than that for UDL.

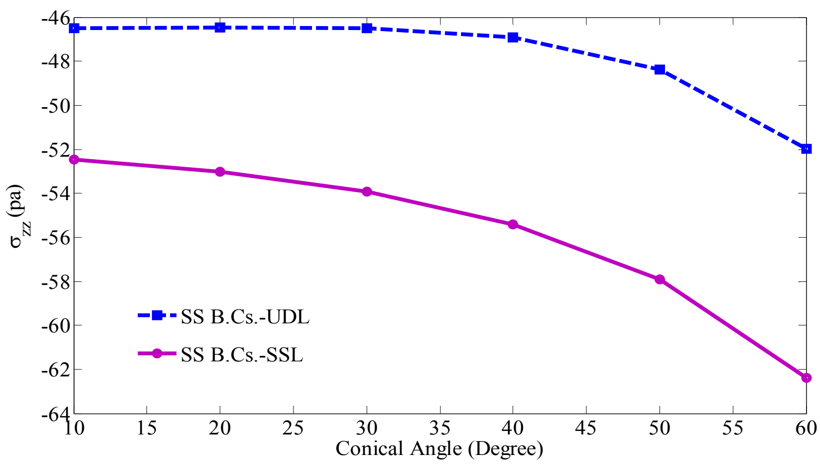

Fig. 5 Variation of transverse normal stress of the core with the conical angles at (x, θ, z_c) = (L/2, 0, h_c/2) for UD and SS loads (q_0 = 100 N)

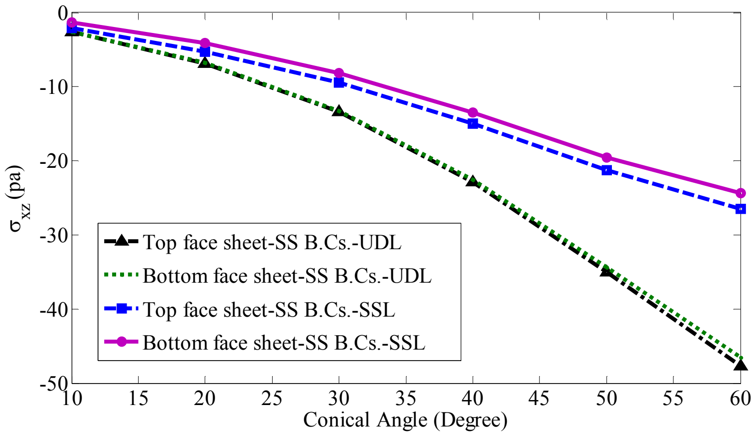

Fig. 6 Variation of transverse shear stress of the face sheets with the conical angles at $(x, \theta, z_i) = (L/2, 0, h_c/2)$, $(i = t, b)$ for UDL and SSL loads (q_0 = 100 N)

Variations of the transverse shear stress of the top and bottom face sheets (σ_{xz}) with the conical angles for a composite conical sandwich panel subjected to SSL and UDL with S.S. B.Cs. at $(x, \theta, z_i) = (L/2, 0, h_c/2)$, $(i = t, b)$ are presented in Fig. 6. As is obvious in this figure, with increasing the conical angle, values of the transverse shear stresses of the face sheets in all the cases were increased. Unlike the transverse normal stress of the core and deflection of the face sheets in Figs. 5 and 4, values of the transverse shear stresses of the face sheets subjected to UDL for all conical angles were much higher than those subjected to SSL. Also, Fig. 6 shows that increasing rate of transverse shear stress of the face sheets with the conical angle for a composite conical sandwich panel subjected to UDL was much higher than that subjected to SSL.

Example 3:
Effect of fiber angle on static response of a composite conical sandwich panel

In this example, effect of the fiber angle on the static response of a composite conical sandwich panel subjected to uniformly (UDL) distributed load with SS and C.C. B.Cs. was investigated. Mechanical and geometrical properties of the composite conical sandwich panel are given in Table 5. Variations of the face sheet deflections with the fiber angles for a composite conical sandwich panel subjected to UDL with SS and C.C. B.Cs. at $(x, \theta, z_i) = (L/2, 0, h_i/2)$, $(i = t, b)$ are presented in Fig. 7. With increasing the fiber angle, values of the dimensionless deflections of the top and bottom face sheets in all the cases decreased and, in the all cases, decreasing rates of deflection were approximately equal, as demonstrated in Fig. 7.

Table 5 Material properties of a conical composite sandwich panel

Foam core	$E_1 = E_2 = E_3 = 0.1036$ GPa, $G_{12} = G_{13} = G_{23} = 0.05$ GPa, $v = 0.036$, $\rho = 130$ kg/m^3
Composite face sheets	$E_1 = 131$ GPa, $E_2 = 10.34$ GPa, $G_{12} = G_{13} = 6.895$ GPa, $G_{23} = 6.205$ GPa, $v_{12} = 0.22$, $\rho = 1627$ kg/m^3
Geometry	$h_c/h = 0.88$, $\phi = 30$, $R_{c1} = 10$ h, $L = R_{c1}$ $[-\theta\ 0\ \theta$ / core / $\theta\ 0\ -\theta]$

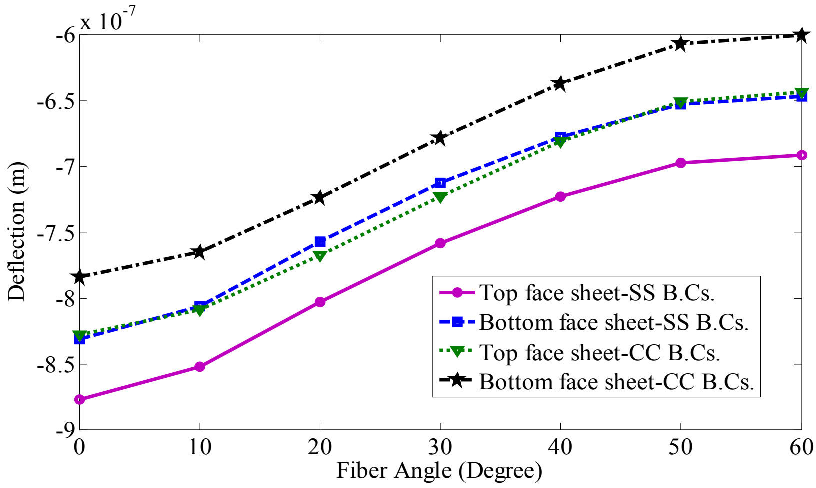

Fig. 7 Variation of dimensionless deflections of the top (outer) and the bottom (inner) face sheet with the fiber angles at $(x, \theta, z_i) = (L/2, 0, h_c/2)$, $(i = t, b)$ for SS and CC B.Cs. ($q_0 = 100$ N)

Furthermore, for both boundary conditions, value of the dimensionless deflection at the center of the bottom face sheet was lower than that at the center of the top face sheet, for the same above-mentioned reason. Variations of the shear stress of the top and bottom face sheets ($\sigma_{x\theta}$) with the fiber angles for a composite conical sandwich panel subjected to UDL with S.S. and C.C. B.Cs. at $(x, \theta, z_i) = (L/2, 0, h_c/2)$, $(i = t, b)$ are presented in Fig. 8. This figure shows that, with increasing fiber angle, variations of the shear stresses ($\sigma_{x\theta}$) for the top face sheet were much higher than those for the bottom face sheet and, for all fiber angles except 0 degree, values of the shear stresses ($\sigma_{x\theta}$) for the top face sheet were much higher than those for the bottom face sheet. Also, Fig. 8 shows that maximum values of the shear stresses ($\sigma_{x\theta}$) for the top face sheet for both boundary conditions occurred in approximately 45 degrees of fiber angle.

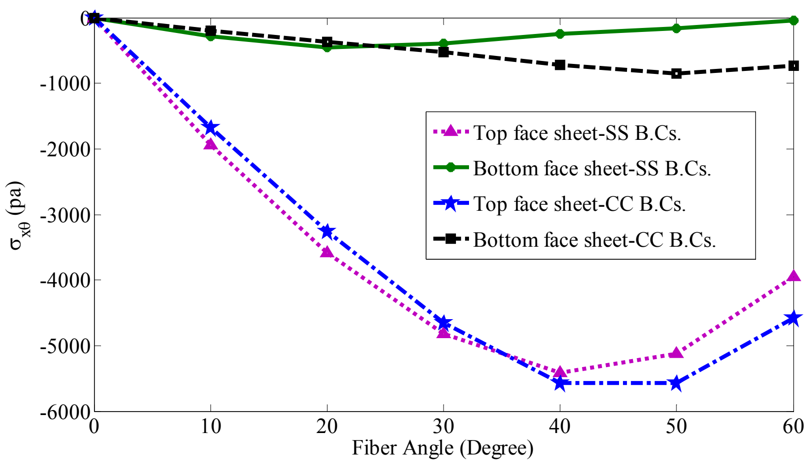

Fig. 8 Variation of $\sigma_{x\theta}$ at $(x, \theta, z_i) = (L/2, 0, h_c/2)$, $(i = t, b)$ with the fiber angles for SS and CC B.Cs. ($q_0 = 100$ N)

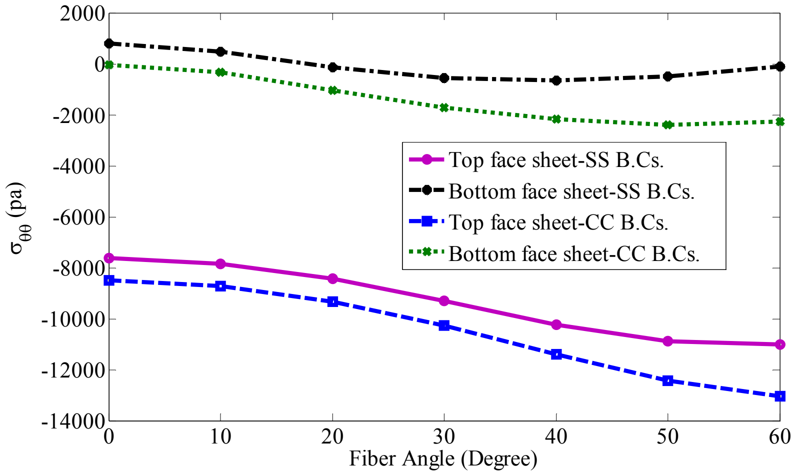

Fig. 9 Variation of $\sigma_{\theta\theta}$ at $(x, \theta, z_i) = (L/2, 0, h_c/2)$, $(i = t, b)$ with the fiber angles for SS and CC B.Cs. ($q_0 = 100$ N)

Variations of the tangential stress of the top and bottom face sheets ($\sigma_{\theta\theta}$) with the fiber angles for a composite conical sandwich panel subjected to UDL with S.S. and C.C. B.Cs at $(x, \theta, z_i) = (L/2, 0, h_c/2)$, $(i = t, b)$ are presented in Fig. 9. Like Fig. 8, Fig. 9 shows that, with increasing the fiber angle, variations of the tangential stress and their values for the top face sheet were much higher than those for the bottom face sheets.

Example 4: Variations of the normal, circumferential and transverse shear stresses and strains through thickness of the core of a truncated conical sandwich panel under a concentrated load

In this example, variations of the normal, circumferential and transverse shear stresses and strains through the thickness direction (along z axis) of the core were studied. The bending analysis of a conical sandwich panel subjected to concentrated load on the top (outer) face sheet with S.S. and C.C. B.Cs. was investigated. Mechanical and geometrical properties of the panel were given in Table 5. The magnitude of concentrated load is 30000 N at point $(x, \theta, z_t) = (L/2, 0, h_t/2)$. Variations of the normal (σ_{xx}) and transverse shear (σ_{xz}) stresses along the thickness direction of the core at $(x, \theta) = (L/4, 0)$ were presented in Fig. 10. This figure shows that, variations of the normal and transverse shear stresses along the thickness direction (z axis) of core for C.C. B.Cs. are a little different. They have nonlinear patterns. It can be observed from this figure that the magnitude of transverse shear (σ_{xz}) stress is more than the magnitude of normal (σ_{xx}) stress in the core and this is a direct consequence of the low shear modulus of the soft core.

Fig. 11 shows variations of the normal (ε_{xx}) and circumferential ($\varepsilon_{\theta\theta}$) strains along z axis in the core under a concentrated load with S.S. B.Cs. at $(x, \theta) = (L/4, 0)$. They have nonlinear patterns.

The results of the presented formulations are validated using results of ABAQUS analysis. In this figure both results of the present analytical and finite element ABAQUS methods were compared with each other. This Figure showed little difference between the results and the presented formulation was in very good agreement with F.E. results. It can be observed from Fig. 11 that the absolute magnitude of circumferential strain is more than the magnitude of normal strain.

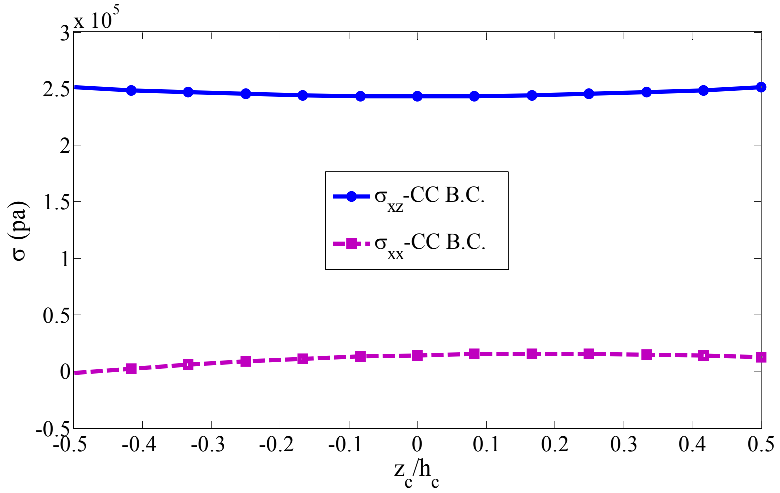

Fig. 10 Variation of the normal and transverse shear stresses along the thickness direction (z axis) of sandwich panel under a concentrated load with C.C. B.Cs. at $(x, \theta) = (L/4, 0)$ ($q_0 = 30000$ N)

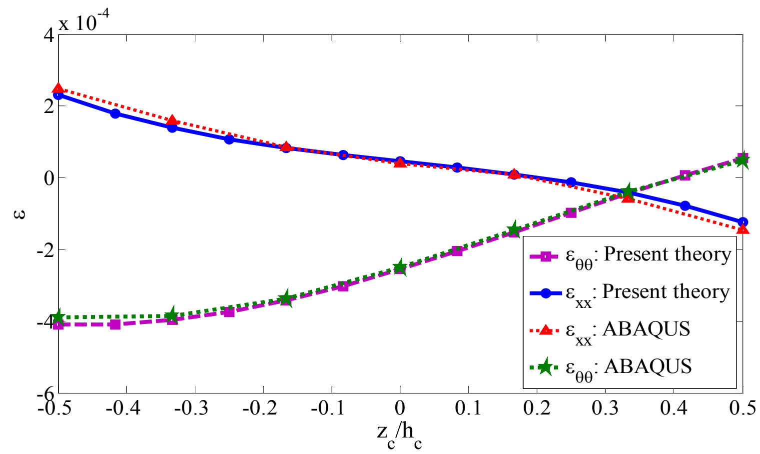

Fig. 11 Variation of the normal (ε_{xx}) and circumferential ($\varepsilon_{\theta\theta}$) strains along the thickness direction (z axis) of sandwich panel under a concentrated load with S.S. B.Cs. at $(x, \theta) = (L/4, 0)$ ($q_0 = 30000$ N)

Variations of the circumferential ($\sigma_{\theta\theta}$) and transverse normal (σ_{zz}) stresses through the thickness direction of the core under a concentrated load with S.S. and C.C. B.Cs. at $(x, \theta) = (L/4, 0)$ were presented in Figs. 12 and 13, respectively.

It can be seen from these figures that the circumferential and transverse normal stresses in the core of conical sandwich panel with S.S. B.Cs. are a little more than those with C.C. B.Cs.. Fig. 12 shows that, the circumferential stress along z axis of the core from the bottom (inner) to the top (outer) interfaces decreases for both boundary conditions while in Fig. 13, the transverse normal stress along z axis of the core from the inner to the outer interfaces increases for both boundary conditions. In Fig. 12 both results of the present analytical and finite element ABAQUS methods were compared with each other. This Figure showed little difference between the results. Therefore, the presented formulation was in very good agreement with F.E. results.

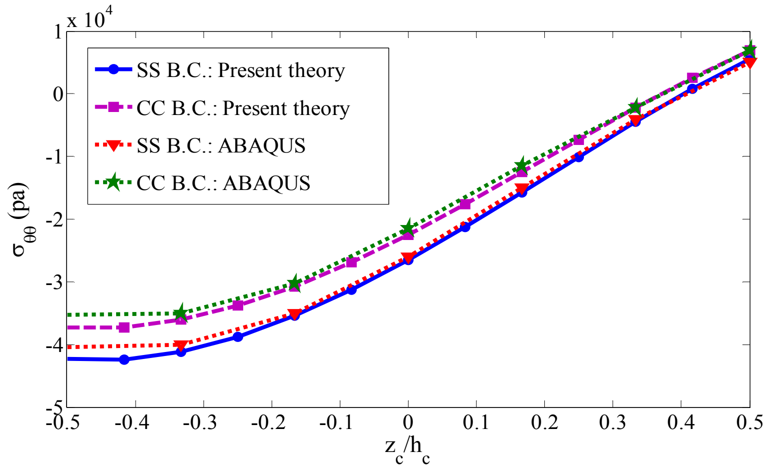

Fig. 12 Variation of $\sigma_{\theta\theta}$ along the thickness direction (z axis) of a sandwich panel under a concentrated load with SS and C.C. B.Cs. at $(x, \theta) = (L/4, 0)$ ($q_0 = 30000$ N)

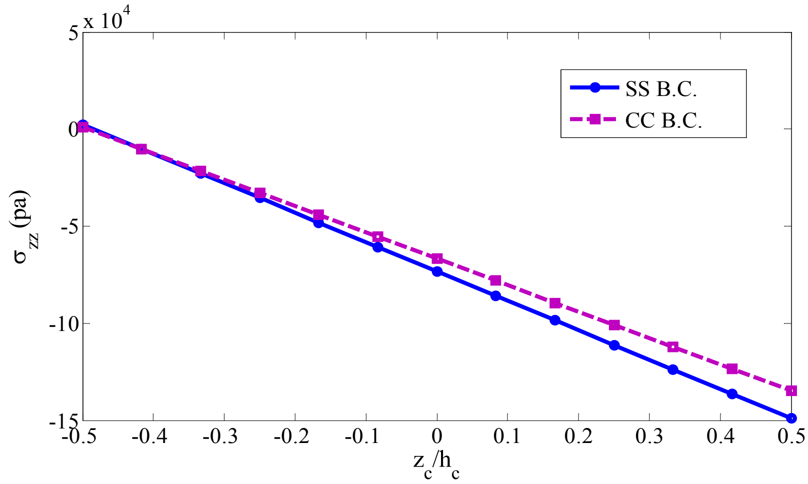

Fig. 13 Variation of σ_{zz} along the core thickness direction (z axis) of a sandwich panel under a concentrated load with SS and C.C. B.Cs. at $(x, \theta) = (L/4, 0)$ ($q_0 = 30000$ N)

5. Conclusions

In this study, bending analysis of a composite conical sandwich panel subjected to various types of applied static loads with S.S. and C.C. B.C.s. was studied. Using the improved higher order sandwich plate theory (IHSAPT) based on the three layers model, the governing equations on the composite conical sandwich panel were derived based on the principle of minimum potential energy. To validate the obtained results, a conical sandwich panel was modeled in ABAQUS F.E. code and the results obtained from analytical formulations and F.E. code were compared with each other. The agreement between these results was very good. Effect of types of boundary conditions, types of applied loads, conical angles and fiber angles on the static bending analysis of truncated conical composite sandwich panels were also studied in detail. The above analysis is quite general and valid for any type of core, any type of boundary conditions, as well as for the cases where the conditions at the top (outer) face sheet are different from those at the bottom (inner) one along the same edge. Similarly, loading may be of any type, distributed or localized. The thickness of the top (outer) face sheet may be different from that of the bottom (inner) face sheet. Transverse shear and rotary inertia effects of face sheets have been taken into consideration.

With increasing the conical angle from 10 to 60 degrees, the dimensionless deflections of the top (outer) and bottom (inner) face sheets in all the cases increased and, in all the cases, increasing rates of deflection were approximately equal. The results show that with increasing the conical angle from 10 to 60 degrees, the magnitudes of the transverse normal stresses in the core increase about 20 percent. The results show that, the circumferential stress along z axis of the core from the inner to the outer interfaces decreases for both simply supported and fully clamped boundary conditions while the transverse normal stress along z axis of the core from the inner to the outer interfaces increases for both boundary conditions. Also, the results show that, with increasing fiber angle, variations of the shear stresses ($\sigma_{x\theta}$) for the outer face sheet were much higher than those for the inner face sheet and, for all fiber angles except 0 degree, values of the shear stresses ($\sigma_{x\theta}$) for the outer face sheet were much higher than those for the inner face sheet. With increasing the fiber angle, variations of the circumferential stress and their values for the outer face sheet were much higher than those for the inner face sheets. Nowadays, in order to optimum design of structures, engineers usually try to minimize the weight and the cost functions and maximize the structural strength function (fitness function) with optimum selecting of the design parameters. Using standard optimization programs like the commercial Genetic algorithm software, one can optimize the design parameters. The present approach can be linked with the standard optimization programs and it can be used in the iteration process of the structural optimization. The proposed approach facilitates investigation of the effect of physical and geometrical parameters on the bending response of sandwich composite structures.

References

Abediokhchi, J., Shakouri, M. and Kouchakzadeh, M.A. (2013), “Bending analysis of moderately thick functionally graded conical panels with various boundary conditions using GDQ method”, *Compos. Struct.*, **103**, 68-74.

Aghdam, M.M., Shahmansouri, N. and Bigdeli, K. (2011), “Bending analysis of moderately thick functionally graded conical panels”, *Compos. Struct.*, **93**(5), 1376-1384.

Bardell, N.S., Langley, R.S., Dunsdon, J.M. and Aglietti, G.S. (1999), “An *h–p* finite element vibration analysis of open conical sandwich panels and conical sandwich frusta”, *J. Sound Vib.*, **226**(2), 345-377.

Bich, D.H., Phuong, N.T. and Tung, H.V. (2012), “Buckling of functionally graded conical panels under mechanical loads”, *Compos. Struct.*, **94**(4), 1379-1384.

Biglari, H. and Jafari, A.A. (2010), “Static and free vibration analyses of doubly curved composite sandwich panels with soft core based on a new three-layered mixed theory”, *J. Mech. Eng. Sci.*, **224**(11), 2332-2349.

Cetkovic, M.D. and Vuksanovic, J. (2009), “Bending, free vibrations and buckling of laminated composite and sandwich plates using a layerwise displacement model”, *Compo. Struct.*, **88**(2), 219-227.

Frostig, Y. and Shenar, Y. (1995), “High-order bending of sandwich beams with a transversely flexible core and unsymmetrical laminated composite skins”, *Compos. Eng.*, **5**(4), 405-414.

Frostig, Y. and Thomsen, O.T. (2004), “Higher-order free vibration of sandwich panels with a flexible core”,

Int. J. Solid. Struct., **41**(5-6), 1697-1724.
He, L., Cheng, Y.S. and Liu, J. (2012), "Precise bending stress analysis of corrugated-core, honeycomb-core and X-core sandwich panels", *Compos. Struct.*, **94**(5), 1656-1668.
Malekzadeh, K., Khalili, S.M.R. and Mital, R.K. (2005), "Local and global damped vibrations of plates with a viscoelastic soft flexible core: An improved high-order approach", *J. Sandw. Struct. Mater.*, **7**(5), 431-456.
Naj, R., Sabzikar Boroujerdy, M. and Eslami, M.R. (2008), "Thermal and mechanical instability of functionally graded truncated conical shells", *Thin-Wall. Struct.*, **46**(1), 65-78.
Nedelcu, M. (2011), "GBT formulation to analyse the buckling behaviour of isotropic conical shells", *Thin-Wall. Struct.*, **49**(7), 812-818.
Pandit, M.K., Sheikh, A.H. and Singh, B.N. (2008), "An improved higher order zigzag theory for the static analysis of laminated sandwich plate with soft core", *Finite Elem. Anal. Des.*, **44**(9-10), 602-610.
Qatu, M.S. (2004), *Vibration of Laminated Shells and Plates*, Elsevier Ltd., Oxford.
Rahmani, O., Khalili, S.M.R. and Malekzadeh, K. (2009), "Free vibration response of composite sandwich cylindrical shell with flexible core", *Compos. Struct.*, **92**(5), 1269-1281.
Reddy, J.N. (2004), *Mechanics of Laminated Composite Plates and Shells*, (2nd Ed.), CRC Press, USA.
Ren-huai, L. and Jun, L. (1995), "Non-linear vibration of shallow conical sandwich shells", *Int. J. Non-Linear Mech.*, **30**(2), 97-109.
Sofiyev, A.H. (2011), "Non-linear buckling behavior of FGM truncated conical shells subjected to axial load", *Int. J. Non-Linear Mech.*, **46**(5), 711-719.
Sofiyev, A.H., Korkmaz, K.A., Mammadov, Z. and Kamanli, M. (2009), "The vibration and buckling of freely supported non-homogeneous orthotropic conical shells subjected to different uniform pressures", *Int. J. Press. Vessels Pip.*, **86**(10), 661-668.
Struk, R. (1984), "Non-linear stability problem of an open conical sandwich shell under external pressure and compression", *Int. J. Non-Linear Mech.*, **19**(3), 217-233.
Stürzenbecher, R., Hofstetter, K. and Eberhardsteiner, J. (2010), "Structural design of Cross Laminated Timber (CLT) by advanced plate theories", *Compos. Sci. Technol.*, **70**(9), 1368-1379.
Stürzenbecher, R. and Hofstetter, K. (2011), "Bending of cross-ply laminated composites: An accurate and efficient plate theory based upon models of Lekhnitskii and Ren", *Compos. Struct.*, **93**(3), 1078-1088.
Wilkins, Jr. D.J., Bert, C.W. and Egle, D.M. (1970), "Free vibrations of orthotropic sandwich conical shells with various boundary conditions", *J. Sound Vib.*, **13**(2), 211-228.
Zhao, X. and Liew, K.M. (2011), "Free vibration analysis of functionally graded conical shell panels by a meshless method", *Compos. Struct.*, **93**(2), 649-664.
Zhen, W. and Wanji, C. (2010), "A C^0-type higher-order theory for bending analysis of laminated composite and sandwich plates", *Compos. Struct.*, **92**(3), 653-661.
Zhong, C. and Reimerdes, H.G. (2007), "Stability behavior of cylindrical and conical sandwich shells with flexible core", *J. Sandw. Struct. Mater.*, **9**(1), 143-166.

CC

Appendix A: Stress resultants per unit length

$$\begin{Bmatrix} N_{xx}^c \\ N_{\theta\theta}^c \\ N_{x\theta}^c \\ N_{\theta x}^c \end{Bmatrix} = \int_{-t_c/2}^{t_c/2} \begin{Bmatrix} \sigma_{xx}^c(1+\dfrac{z_c}{R_{c_0}+x\sin(\phi)}) \\ \sigma_{\theta\theta}^c \\ \sigma_{x\theta}^c(1+\dfrac{z_c}{R_{c_0}+x\sin(\phi)}) \\ \sigma_{x\theta}^c \end{Bmatrix} dz_c, \begin{Bmatrix} M_{nxx}^c \\ M_{n\theta\theta}^c \\ M_{nx\theta}^c \\ M_{n\theta x}^c \end{Bmatrix} = \int_{-t_c/2}^{t_c/2} z_c^n \begin{Bmatrix} \sigma_{xx}^c(1+\dfrac{z_c}{R_{c_0}+x\sin(\phi)}) \\ \sigma_{\theta\theta}^c \\ \sigma_{x\theta}^c(1+\dfrac{z_c}{R_{c_0}+x\sin(\phi)}) \\ \sigma_{x\theta}^c \end{Bmatrix} dz_c,$$

$$\begin{Bmatrix} N_{xz}^c \\ N_{\theta z}^c \\ M_{nxz}^c \\ M_{n\theta z}^c \end{Bmatrix} = \int_{-t_c/2}^{t_c/2} \begin{Bmatrix} \sigma_{xz}^c(1+\dfrac{z_c}{R_{c_0}+x\sin(\phi)}) \\ \sigma_{\theta z}^c \\ z_c^n\sigma_{xz}^c(1+\dfrac{z_c}{R_{c_0}+x\sin(\phi)}) \\ z_c^n\sigma_{\theta z}^c \end{Bmatrix} dz_c, \begin{Bmatrix} N_{xz}^{*c} \\ N_{\theta z}^{*c} \\ M_{nxz}^{*c} \\ M_{n\theta z}^{*c} \end{Bmatrix} = \int_{-t_c/2}^{t_c/2} \begin{Bmatrix} \sigma_{xz}^c \\ \sigma_{\theta z}^c \\ z_c^n\sigma_{xz}^c \\ z_c^n\sigma_{\theta z}^c \end{Bmatrix} (1+\dfrac{z_c}{R_{c_0}+x\sin(\phi)}) dz_c,$$

$$R_z^c, M_z^c = \int_{-t_c/2}^{t_c/2} (1,z_c)\sigma_{zz}^c(1+\dfrac{z_c}{R_{c_0}+x\sin(\phi)})dz_c, \quad \begin{Bmatrix} N_{xx}^i \\ N_{\theta\theta}^i \\ N_{x\theta}^i \\ N_{\theta x}^i \end{Bmatrix} = \int_{-d_i/2}^{d_i/2} \begin{Bmatrix} \sigma_{xx}^i \\ \sigma_{\theta\theta}^i \\ \sigma_{x\theta}^i \\ \sigma_{x\theta}^i \end{Bmatrix} dz_i,$$

$$\begin{Bmatrix} M_{xx}^i \\ M_{\theta\theta}^i \\ M_{x\theta}^i \\ M_{\theta x}^i \end{Bmatrix} = \int_{-d_i/2}^{d_i/2} z_i \begin{Bmatrix} \sigma_{xx}^i \\ \sigma_{\theta\theta}^i \\ \sigma_{x\theta}^i \\ \sigma_{x\theta}^i \end{Bmatrix} dz_i, \quad \begin{Bmatrix} Q_{xz}^i \\ Q_{\theta z}^i \end{Bmatrix} = k_s \int_{-d_i/2}^{d_i/2} \begin{Bmatrix} \sigma_{xz}^i \\ \sigma_{\theta z}^i \end{Bmatrix} dz_i \ ; \ i = t,b \text{ and } n = 1,2,3.$$

Appendix B: Some coefficients of stiffness matrix

$$K(3,15)=-\frac{2q}{h_c^2}\left(-e_2^{c\theta\theta}+4\frac{e_4^{c\theta\theta}}{h_c^2}\right)\pi T_4-\frac{4}{h_c^3}\left(-e_3^{c\theta\theta}+4\frac{e_5^{c\theta\theta}}{h_c^2}\right)\pi T_4-\frac{2q}{h_c^2}\left(-H_3^{c\theta z}+4\frac{H_5^{cxz}}{h_c^2}\right)\pi T_4$$
$$-\frac{4q}{h_c^3}\left(-H_4^{c\theta z}+4\frac{H_6^{cxz}}{h_c^2}\right)\pi T_4+\frac{4q}{h_c^2}\left(-g_1^{c\theta z}+4\frac{g_3^{cxz}}{h_c^2}\right)\pi T_3+\frac{12q}{h_c^3}\left(-g_2^{c\theta z}+4\frac{g_4^{cxz}}{h_c^2}\right)\pi T_3$$

$$K(7,14)=\frac{h_t q\sin(\phi)}{h_c^2}\left(e_3^{c\theta\theta}-4\frac{e_5^{c\theta\theta}}{h_c^2}\right)\pi T_6+\frac{2h_t q\sin(\phi)}{h_c^3}\left(e_4^{c\theta\theta}-4\frac{e_6^{c\theta\theta}}{h_c^2}\right)\pi T_6-\frac{qh_t}{h_c^2}\left[\alpha_m\left(g_3^{c\theta x}-4\frac{g_5^{c\theta x}}{h_c^2}\right)\pi T_2\right.$$
$$\left.-\sin(\phi)\left(-H_3^{c\theta x}+4\frac{H_5^{c\theta x}}{h_c^2}\right)\pi T_6\right]-\frac{2qh_t}{h_c^3}\left[\alpha_m\left(g_4^{c\theta x}-4\frac{g_6^{c\theta x}}{h_c^2}\right)\pi T_2-\sin(\phi)\left(-H_4^{c\theta x}+4\frac{H_6^{c\theta x}}{h_c^2}\right)\pi T_6\right]$$

$$K(14,5)=-\frac{q}{h_c}\left(e_2^{c\theta\theta}-4\frac{e_4^{c\theta\theta}}{h_c^2}\right)\pi T_4-\frac{2}{h_c^2}\left(e_3^{c\theta\theta}-4\frac{e_5^{c\theta\theta}}{h_c^2}\right)\pi T_4+\frac{q}{h_c}\left[\left(-H_2^{c\theta z}+4\frac{H_4^{c\theta z}}{h_c^2}\right)\pi T_4+\right.$$
$$\left.\alpha_m^2\left(g_1^{c\theta z}-12\frac{g_3^{c\theta z}}{h_c^2}\right)\pi T_3\right]+\frac{2q}{h_c^2}\left[\left(-H_3^{c\theta z}+4\frac{H_5^{c\theta z}}{h_c^2}\right)\pi T_4+\alpha_m^2\left(g_2^{c\theta z}-12\frac{g_4^{c\theta z}}{h_c^2}\right)\pi T_3\right]$$

where

$$T_1=\frac{2}{L}\int_0^L\frac{\cos(\alpha_m x)\cos(\alpha_p x)}{R(x)}dx,\ T_2=\frac{2}{L}\int_0^L\frac{\cos(\alpha_m x)\cos(\alpha_p x)}{R^2(x)}dx,\ T_3=\frac{2}{L}\int_0^L\frac{\sin(\alpha_m x)\sin(\alpha_p x)}{R(x)}dx,$$
$$T_4=\frac{2}{L}\int_0^L\frac{\sin(\alpha_m x)\sin(\alpha_p x)}{R^2(x)}dx,\ T_5=\frac{2}{L}\int_0^L\frac{\sin(\alpha_m x)\cos(\alpha_p x)}{R(x)}dx,\ T_6=\frac{2}{L}\int_0^L\frac{\sin(\alpha_m x)\cos(\alpha_p x)}{R^2(x)}dx,$$
$$T_7=\frac{2}{L}\int_0^L\frac{\cos(\alpha_m x)\sin(\alpha_p x)}{R(x)}dx,\ T_8=\frac{2}{L}\int_0^L\frac{\cos(\alpha_m x)\sin(\alpha_p x)}{R^2(x)}dx,\ T_9=\frac{2}{L}\int_0^L\frac{\sin(\alpha_m x)\cos(\alpha_p x)}{R^3(x)}dx,$$
$$T_{10}=\frac{2}{L}\int_0^L\frac{\sin(\alpha_m x)\sin(\alpha_p x)}{R^3(x)}dx,\ T_{11}=\frac{2}{L}\int_0^L\frac{\cos(\alpha_m x)\sin(\alpha_p x)}{R^3(x)}dx,\ T_{12}=\frac{2}{L}\int_0^L\frac{\sin(\alpha_m x)\sin(\alpha_p x)}{R^4(x)}dx,$$
$$T_{13}=\frac{2}{L}\int_0^L\frac{\cos(\alpha_m x)\sin(\alpha_p x)}{R^4(x)}dx,\ T_{14}=\frac{2}{L}\int_0^L\frac{\cos(\alpha_m x)\cos(\alpha_p x)}{R^3(x)}dx,\ T_{15}=\frac{2}{L}\int_0^L\frac{\cos(\alpha_m x)\cos(\alpha_p x)}{R^4(x)}dx,$$
$$T_{16}=\frac{2}{L}\int_0^L\frac{\sin(\alpha_m x)\cos(\alpha_p x)}{R^4(x)}dx,$$
$$T_{3i}=\frac{2}{L}\int_0^L\frac{\sin(\alpha_m x)\sin(\alpha_p x)}{R_{i1}(x)}dx,\ T_{4i}=\frac{2}{L}\int_0^L\frac{\sin(\alpha_m x)\sin(\alpha_p x)}{R_{i1}^2(x)}dx,\ T_{7i}=\frac{2}{L}\int_0^L\frac{\cos(\alpha_m x)\sin(\alpha_p x)}{R_{i1}(x)}dx,\ i=t,b$$
$$\int_0^L\cos(\alpha_m x)\cos(\alpha_p x)dx=\int_0^L\sin(\alpha_m x)\sin(\alpha_p x)dx=\frac{L}{2},\int_0^L\cos(n\theta)\cos(q\theta)dx=\int_0^L\sin(n\theta)\sin(q\theta)dx=\pi.$$